Edge Diffraction and Surface Scattering in Concert Halls: Physical and Perceptual Aspects

Rendell R. Torres, Nicolas de Rycker and Mendel Kleiner

Program in Architectural Acoustics, Rensselaer Polytechnic Institute Greene Building, 110 8th St., Troy, New York, 12180-3590USA

(Received 15 October 2003; revised 5 June 2004; accepted 31 August 2004)

In auralization of room sound fields, most conventional approaches base their computations on geometrical-acoustics assumptions, which fail at lower frequencies (or for scattering from small facets) due to the neglect of edge diffraction and to coarse approximations of surface scattering, e.g., approximations based on Lambert-scattering models. This paper investigates the physical and subjective effects of three main approaches to modeling surface scattering for inclusion in transient room impulse responses for auralization, as the impulse response is the temporal characteristic of the roomís acoustical quality. These scattering models include the following: Lambert surface scattering from rough surfaces, edge-diffraction, and boss surface-scattering. In particular, a parametric approach to modeling edge-diffraction is developed and compared with the high-accuracy model; the parametric approach uses four output parameters to collectively model the physical behavior of edge diffraction and retains the phase effects that reproduce the basic first-order scattering behavior from finite facets.

Keywords: auralization, scattering, diffraction, edge diffraction, perceptual modeling, physical modeling

INTRODUCTION

For the acoustical analysis and design of rooms, acousticians often rely on room-acoustics simulation software based on geometrical-acoustics principles, i.e., that acoustical wavefronts can be modeled as rays (or propagation from image sources) that reflect from faceted surfaces, thus yielding the temporal pattern of reflection known as the echogram. Such tools are attractive because they offer calculation of room-acoustics parameters from computed echograms. In addition, by assigning phase (e.g., minimum phase) to reflections, many typical commercial algorithms can generate impulse responses for auralization, i.e., the binaural simulation of a virtual or physical acoustic environment.

Among the approximations inherent to such programs, however, one of the most significant is the treatment of surface scattering. Non-specular surface scattering can essentially be divided into two main types: edge diffraction and surface scattering, which both affect the perceived coloration and spaciousness of a given sound field [1,2]. Inadequate modeling of surface scattering can lead to inaccuracies in auralization. Depending on the required level of accuracy, however, different scattering models may be appropriate. This paper discusses various numerical models, as well as their suitability for a given application. Although there are several algorithms that may be used to compute room sound fields, this discussion focuses on specific time-domain models for edge-diffraction and boss-scattering [3-5] that are well-suited to complementing current, most commonly used algorithms that are based on geometrical acoustics principles. Moreover, this paper focuses more on the effects of the physical and subjective phenomena than on the numerical models themselves.

a) Electronic mail: rrtorres@rpi.edu

1.LAMBERTSCATTERINGMODELS

Geometrical-acoustics models have limited utility but still give useful information at higher frequencies where the wavelength is less than about 1/10 the smallest projected dimension of a reflecting surface facet. In these models the reflection energy is determined by a frequency-dependent absorption coefficient (approximated typically as a random-incidence, angular-independent value). The calculated reflection density depends also on the assumed wall scattering coefficient, where the scattering is commonly modeled using a tessellation of Lambert sources that simulate a rough scattering surface [6, 7].

Lambert-models for surface scattering are useful for approximately simulating scattering from randomly rough surfaces; moreover, to predict basic reverberation decays,

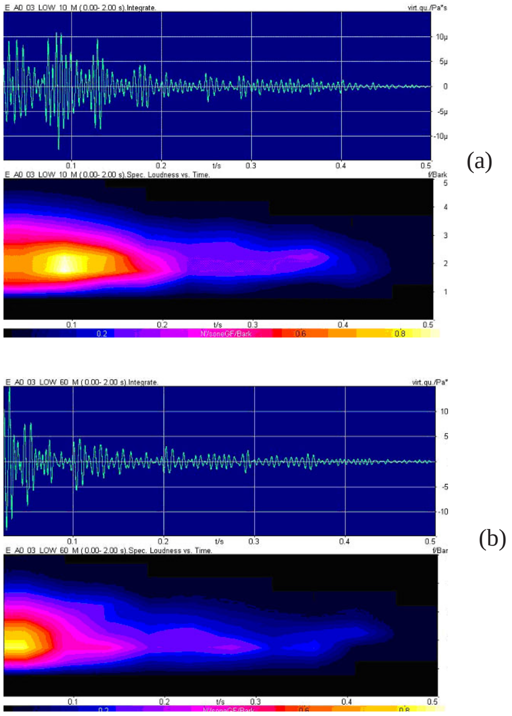

Fig. 1. The effects of changing the scattering coefficient are depicted by two pairs of plots showing the impulse response (band-pass filtered at the 125- and 250-Hz octave bands) and the specific loudness vs. time (500 ms) and critical band. Figures (a) and (b) correspond to scattering coefficients of 10% and 60%, respectively. When the scattering coefficient increases, as in Fig. 1(b), the reflection-peaks in the impulse response decrease. The loudness level contours in Fig. 1(b) also reveal the conversion of specularly reflected energy to diffusely scattered energy.

Lambert-scattering models yield significant improvements over algorithms based on geometrical acoustics without any scattering models at all [8-12].

For computing higher-resolution impulse responses for auralization, however, Lambert-scattering models can only represent gross effects of surface scattering and not fine details that create, e.g., audible differences in timbre. Some major limitations of a Lambert-based scattering model are that (1) it does not simulate well the complex scattering directivity from two-dimensional scattering geometries such as edges of finite planes and cylinders, and (2) it neglects phase, thus neglecting interference effects between specular and non-specular scattering, whose sum constitutes the total surface scattering at a receiver position in a room. This latter effect is especially important at non-specular angles of surface scattering to the receiver. Although it would be clearly advantageous to improve auralization algorithms to model phase more accurately both in the absorption coefficient and in the surface scattering, the discussion of this paper will limit itself to the latter.

Nevertheless, despite its oversimplification of surface scattering, Lambert-scattering can still function as a perceptually-based approximation to surface scattering where phase is neglected. To illustrate the effects of changing the Lambert-scattering coefficient in a room, Figure 1 plots the computed impulse response of a concert hall (from Ref. [1]) and specific loudness spectrogram (vs. time and critical band, i.e., the bandwidth resolution of human hearing [14]) for two different values of the Lambert scattering coefficient (10% and 60%) in the frequency region covered by the 125-250 Hz octave bands. The plots illustrate how the increase in the scattering coefficient decreases the amplitude of early reflections, time-smears the non-specular scattered energy, and changes the relative balance between direct, reflected, and reverberant energy.

Figure 2 shows previous results of listening tests [1] that investigated the perceived difference in changes of the Lambert scattering coefficient from 10% to 60% over different frequency ranges. These figures showed that changes in scattering coefficient are audible in all frequency regions tested, where the relative audibility is related to the input signal. Moreover, Ref [1] showed that for perceptual (i.e., aural) accuracy, scattering must be treated with frequency dependence (not all auralization programs do this), and with models appropriate to each frequency (see also [13]).

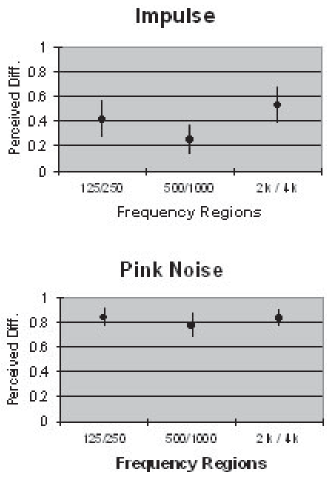

Fig. 2. Results from pair comparison listening tests, where subjects rated the ì Perceived differencesî resulting from changes in Lambert scattering coefficients from 10% to 60%. [1] Subjects were not told how the auralizations differed, but they were given reference auralizations as ì anchor pointsî that represented values of 1 (1 = clear audible difference; 0 = no audible difference).

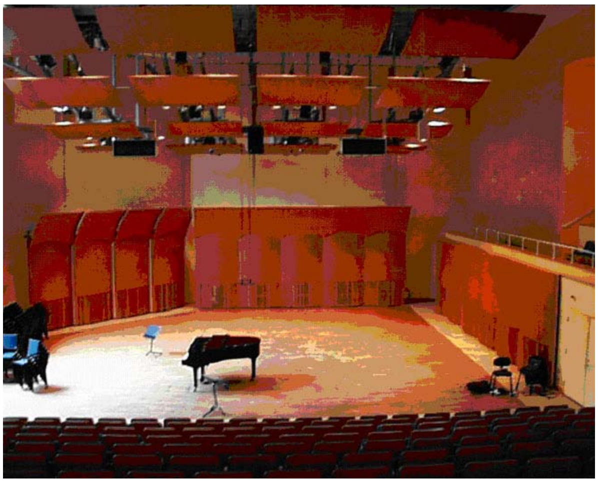

Fig. 3. Scattering from edges of finite planes in the conservatory Musikhogskolan, Goteborg, Sweden. (Photo: M. Kleiner)

2. EDGE DIFFRACTION

2.1. High-accuracy computations

Edge diffraction is the first major correction to geometrical acoustics and the corresponding assumption that all reflecting surfaces are rigid and infinite in extent [2,3]. Figure 3 shows a performance hall environment (at the Music Conservatory in Gothenburg, Sweden) with several dedicated reflector panels, modeled as finite-size facets whose scattering is significantly non-specular at long wavelengths.

In order to minimize the computational demands of including scattering in auralization, it is appropriate to study how many orders of scattering need to be included. For this purpose, studying edge diffraction is especially appropriate, since edge diffraction can be considered an elementary form of surface scattering. In a previous study incorporating edge-diffraction computations and listening tests [2], it was found that higher orders and combinations of edge diffraction components were not usually as significant as first-order diffraction components when the receiver was visible to the source. Additionally, the total diffraction effects within the audible frequency range were relatively small above about 150 Hz. The reason for this was that the reference geometry (a large concert-hall stagehouse) was conservatively composed of large flat walls whose dimensions were larger than most of the wavelengths of interest. This was ìconservativeî in the sense that only the longest wavelengths of interest would give rise to significant edge-diffractions, and the study investigated whether in such cases the diffraction was audible in listening tests. The results interestingly showed that these diffraction effects were still audible for various input signals.

More realistic reflecting surfaces in rooms, however, do not primarily consist of large, bare walls but more often include smaller-scale surface irregularities, e.g., facets for which audible wavelengths are typically a similar order or larger. A variety of such elements is shown in Fig. 3, where the boundaries of various reflecting surfaces gives rise to edge diffraction, or scattering from the edges of the finite-size panels. To most clearly illustrate the effect of calculating varying orders of diffraction, we initially consider the scattering (reflection + diffraction) from a single rectangular panel. Figure 4 shows an elevation of the source-panel-receiver configuration.

Figure 5 shows the difference between calculations (using the edge-diffraction model by Svensson et al. [3]) including up to first-order and calculations including up to second-order diffraction. It is clear that second-order diffraction must be included when the wavelength is approximately greater than five times the projected width (i.e., at low frequencies) and

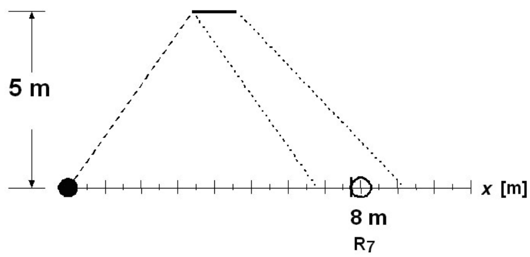

Fig. 4. Geometry of edge-diffraction computation.

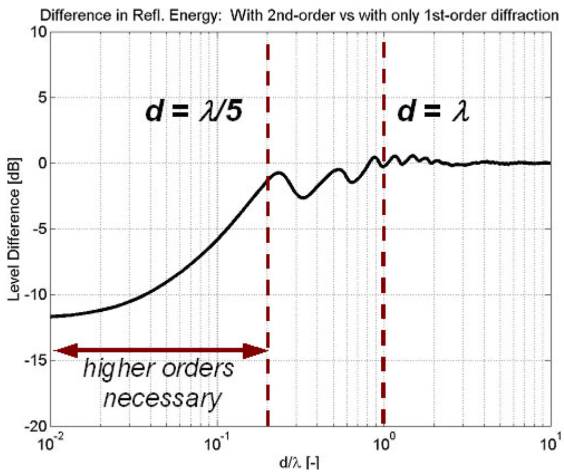

Fig. 5. Error in neglecting second- (and higher-) order diffraction. When the wavelength exceeds approximately five times the panel width, first-order diffraction computations are insufficient, and one must compute higher orders of diffraction.

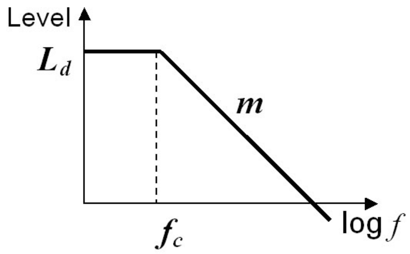

Fig. 6. Illustration of simplified low-pass filters to parametrically model edge-diffraction.

that successively higher orders are needed. However, within and above the transition zone (indicated by dotted lines), first-order diffraction appears adequate to model the total scattering from the panel for this somewhat generic source-receiver configuration.

2.2. Perceptual approximations to edge diffraction

One can construct perceptual approximations to edge diffraction by describing (and then modeling) edge-diffraction parametrically by physical phenomena. We do this by computing simplified finite impulse response (FIR) filters, e.g., for medium-resolution virtual-reality applications. Our six input parameters are the source and receiver positions (each described by two cylindrical coordinates), the wedge angle (e.g., $\theta_w = 0$ corresponds to a knife-edge and $\theta_w = \pi$ to a half-plane), and the wedge length. The four output parameters that describe the diffraction are the level L_d, ìcutoff frequencyî f_c of the diffraction (which resembles a low-pass filter, as depicted in Fig. 6), slope m of the response above the cutoff frequency, and the phase/polarity of the diffraction (which, for a given finite plane, controls how the diffraction constructively or destructively interferes with the specular reflection from that plane). First-order diffraction drops off above the cutoff frequency f_c at a rate of about –3 dB/octave; higher orders drop off at approximately –6 dB/octave, –9 dB/octave, etc.

In particular we examine (1) the directivity functions of the scattering around the edge, (2) the frequency spectra of this scattering and the dependence on distance (to determine whether it follows a far-field type of behavior), and (3) wedge length (to determine the effect of the wedge at lower frequencies/longer wavelengths).

Figure 7 shows the directivity and polarity of the edge-scattering functions as a function of angle from the edge of a semi-infinite plane. There are three zones corresponding to the existence of the direct sound (Zone I and II), specular reflections (Zone I), and diffraction alone (in the Zone III ìshadowî region). The directivity plot and frequency responses show that there are singularities in the computed edge diffraction at the zone boundaries, but a continuous total sound field when all pressure components, i.e., edge diffraction components and specular components, are summed together. The frequency spectra in Fig. 8 also show how the diffraction resembles a low-pass filter to varying degrees depending on the zone. In Fig. 8-10, the reference 0 dB signifies the level of a specular (geometrical) reflection from the surface without accounting for edge diffraction.

The frequency response of the total scattering from the panel (edge diffraction + specular reflection) is shown in Fig. 9. Even though the edge diffraction is discontinuous at the zone boundaries of the sound field (i.e., the boundaries where the specular reflection and direct sound disappear, respectively

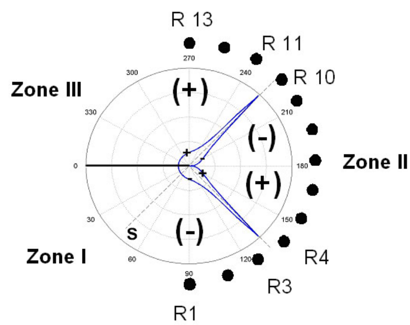

Fig. 7. Directivity and polarity of first-order edge diffraction. The solid circles represent receiver positions R1 through R13 where the impulse response (including reflection and diffraction) is calculated. The positive and negative signs refer to the polarity/phase of the diffraction impulse response. Zones I, II, and III refer to areas as described in the text.

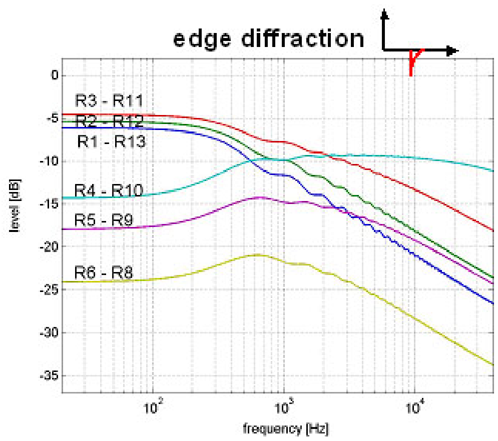

Fig. 8. Frequency response of edge-diffraction as a function of scattering angle at several receiver positions around the edge. The labels R1 to R11 correspond to the receiver positions depicted in Fig. 7.

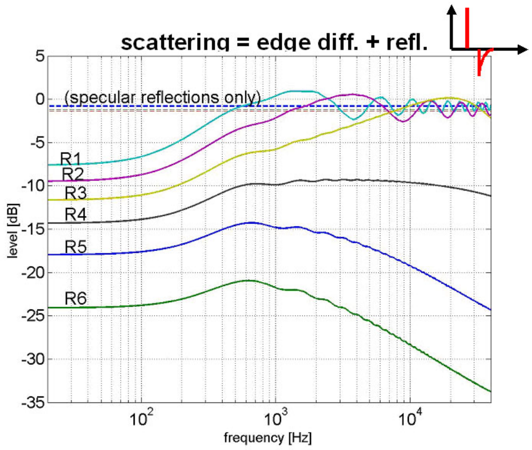

Fig. 9. Frequency response of total scattering (edge diffraction + specular reflection). Even though the edge diffraction is discontinuous at the zone boundaries, the total scattering shown here is smoothly varying, as one would expect for a continuous sound field. The labels R1 to R6 correspond to the receiver positions depicted in Fig. 7.

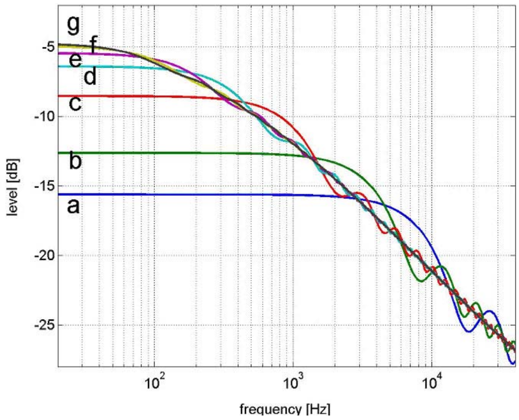

Fig. 10. Variation with wedge length: a = 0.2 m, b = 0.3 m, c = 0.6 m, d = 1.05 m, e = 1.6 m, f = 2.4 m, g = 3.0 m. Wedge angle = 20 degrees; rec. angle = 60 degrees. The results show that longer wedges contribute stronger edge diffraction at lower frequencies; therefore, when using simplified description of edge diffraction, one cannot neglect wedge length (e.g., as one does when using the geometrical theory of diffraction).

[2]), the total scattering shown here is smoothly varying, as one would expect for a continuous sound field.

The results in Fig. 10 show that longer wedges contribute stronger edge diffraction at lower frequencies; therefore, when using simplified description of edge diffraction, one cannot neglect wedge length (e.g., as one does when using the geometrical theory of diffraction). The computations for Fig. 10 were done for wedge lengths of a = 0.2 m, b = 0.3 m, c = 0.6 m, d = 1.05 m, e = 1.6 m, f = 2.4 m, g = 3.0 m. The wedge angle is 20 degrees, and the receiver position is at 60 degrees. This effect (of greater edge diffraction for longer wedges) is typical for various source positions.

If one approximately models the edge-diffraction as a simple low-pass FIR filter and superposes this with the specular reflection, this approximation of the total scattering may be compared to a higher accuracy computation. This comparison is shown in Fig. 11. It is important that the polarity of the diffraction impulse response is correct, since the total scattering must reflect the correct interference among the individual (direct, reflected, and diffracted) components. Figure 11 shows that the total scattering seems to be modeled relatively well, with up to 3 dB errors for this source, receiver, and edge configuration. This is an encouraging result, as it demonstrates that one may feasibly use such simplified models of edge diffraction for applications where the highest accuracy is not required (e.g., for fast virtual-reality computations).

3. BOSS-MODEL SURFACE SCATTERING

Edge-diffraction models are not optimized, however, to model scattering from individual scatterers such as spheres. Such scattering can be calculated using so-called boss models, where a boss is simply a protuberance from a surface. We present here some initial calculations and results in this area.

Figure 12 shows the simulated listener orientation relative to the two walls for which the scattering is calculated according to Fig. 13. The non-specular scattering from the sphere is calculated according to the image-implementation of the classical solution for scattering from spheres [4,5], as

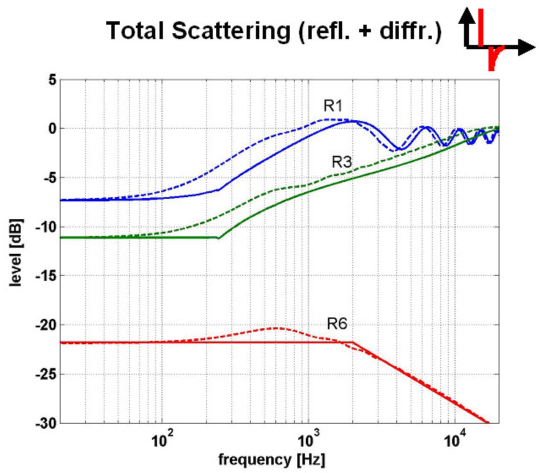

Fig. 11. Frequency response of total scattering (reflection + edge diffraction). The dotted lines represent the high-accuracy solution; the solid lines depict the parametric approximation.

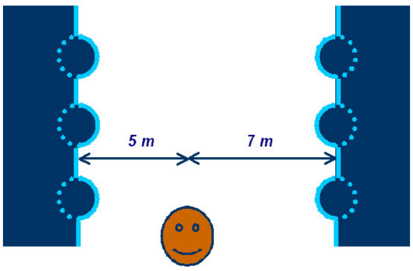

Fig. 12. Orientation of listener/receiver position for boss-scattering calculation and auralizations. The listener was positioned off axis between two walls with scattering bosses (protuberances from the flat surface).

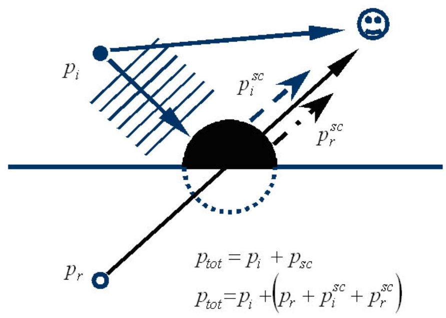

Fig. 13. The total scattering p_{sc} from a hemispherical boss is modeled as the sum of three terms: the planar ″specular″ reflection p_r, and the scattering of incident and reflected sound p_i^{sc} and p_r^{sc} from a sphere with the same diameter.

illustrated in Fig. 13 for one hemispherical boss on an infinite rigid plane. Here, the total sound field is regarded as a sum of the direct sound p_i and the scattered sound p_{sc}, which itself is composed of the ì specularî (image-like) reflection from the flat plane p_r and the ì non-specularî boss-scattering of the incident and reflected sound, p_i^{sc} and p_r^{sc}.

The calculation details are as follows. The sphere diameters were varied uniformly to be 0.1, 0.23, and 0.37 m. Only scattering from two side walls (with areas 10 x 10 meters each and separated by a 12 m distance) were calculated, with bosses evenly spaced at densities of 2x3, 5x3, and 8x8 bosses per side wall. As a third parameter, the boss positions were dithered in the 8x8 case. The sound source was a point source, and the point receiver was located 5 meters from one side wall and 7 meters from the other.

Figures 14 and 15 show results from these calculations, where only first-order non-specular scattering is included. In particular, the early decay and level of the reverberation is clearly dependent on the boss number and size. Initial listening tests (pair comparisons) with multi-dimensional scaling of the results indicate that variations in either of these factors (boss size and boss density) are statistically significant in causing audible changes in the binaural room impulse response. One should also recall that only first-order scattering was included here (and the boss positions were relatively sparse with respect to wavelength) and note that the inclusion of coupled scattering (higher-order interactions) among bosses will also affect the spectral and spatial character of the boss surface scattering, especially as the bosses increase in number and density (i.e., proximity to each other).

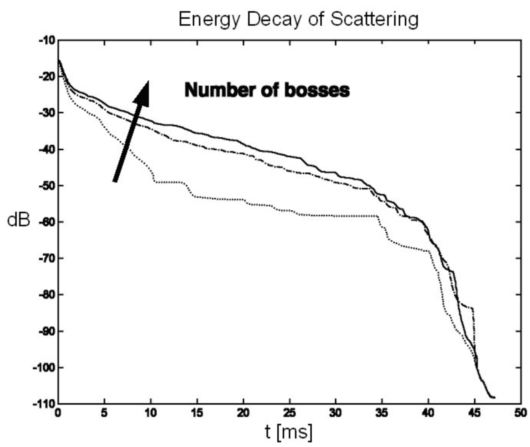

Fig. 14. Early energy decay for various boss densities. The ì number of bossesî corresponds to the boss densities of 2x3, 5x3, and 8x8 bosses per side wall.

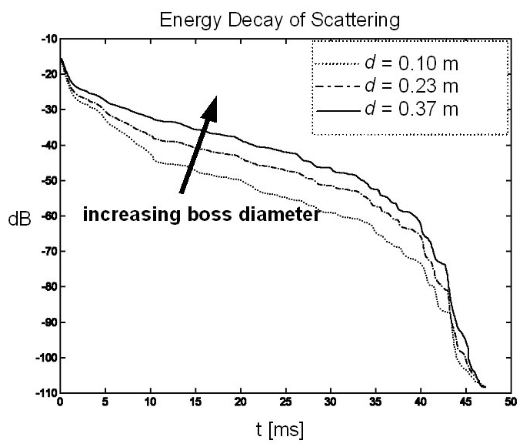

Fig. 15. Early energy decay for different boss sizes.

4. CONCLUSIONS AND FUTURE WORK

Construction of simplified scattering filters based on few parameters may make faster computation of edge diffraction possible for virtual-reality, medium-resolution applications. Future work will be needed to determine how to optimally determine the parametrical outputs for the simplified diffraction filters (e.g., using look-up tables or neural networks). Additional numerical investigation and subjective testing is also needed to determine how best to model parametrically scattering from hemispherical bosses [15]. Finally, one should investigate how to characterize spatial and timbral effects of scattering and to what extent different amounts of reverberation masks or otherwise affects such perceptual effects in the early room impulse response. When one listens to continuous or repetitive signals, the reverberation from an earlier part of the input signal can mask a later part of the input signal, just as reverberation can mask or muddle speech. In such a case, the timbre (influenced by early reflections) of the voice is changed, or at least partially masked, by increasing the reverberation. In addition, when reverberation is present, the listener may partially be distracted by the reverberation and not concentrate as closely on the timbral and spatial effects of the early reflections.

5.REFERENCES

[1] Torres, R. R., Kleiner, M. and Dalenback, B.-I. (2000). Audibility of ëdiffusioní in room acoustics auralization: an initial investigation. Acustica/Acta Acustica 86, 919-927.

[2] Torres, R. R., Svensson, U. P., and Kleiner, M. (2001). Computation of edge diffraction for more accurate room acoustics auralization. J. Acoust. Soc. Am. 109, 600-610.

[3] Svensson, U. P., Fred, R. I. and Vanderkooy, V. (1999). An analytic secondary source model of edge diffraction impulse responses. J. Acoust. Soc. Am. 106, 2331-2344.

[4] Torres, R. R., Kleiner, M. and Natsiopoulos, G. (2001) Room acoustics auralization studies of laterally incident boss-model scattering. J. Acoust. Soc. Amer., Nov 2001, (A).(Mtg. of the Acoustical Society of America, Dec. 2002)

[5] Natsiopoulos, G. (2000). Studies of Analytical Models for Spherical and Cylindrical Scattering. M.Sc. thesis, Report E 00-05, ISSN 0283-8338, Dept. of Applied Acoustics, Chalmers Univ. Tech., Gothenburg, Sweden.

[6] Dalenback, B.-I. (2002). CATT-Acoustic v8 Userís Manual. published by CATT.

[7] Kuttruff, H. (1991). Room Acoustics, 3rd Ed., Applied Science Publishers Ltd., New York, p. 84.

[8] Vorlander, M. (1995). International round-robin on room acoustical computer simulations. Proceedings of the 15th Intl. Congress on Acoustics, Trondheim, Norway, pp. 689-692.

[9] Bork, I. (2000). A comparison of room simulation software ? The 2nd Round Robin on room acoustical computer simulation. Acustica/Acta Acustica 86, pp. 943-956.

[10] Bork, I. (2002). Simulation and measurement of auditorium acoustics - The round robins on room acoustical simulation. Proceedings of the Institute of Acoustics, Vol. 24, Part 4, London, (ISBN 1 901656 47 0)

[11] Torres, R. R. Studies of Edge Diffraction and Scattering: Applications to Room Acoustics and Auralization, doctoral thesis, ISBN 91-7197-965-5, Chalmers Univ. of Tech., Sweden.

[12] Hodgson, M. (2000). Evidence of diffuse surface feflections in fooms. J. Acoust. Soc. Am. 89(2), 765-771 (1991).

[13] Embrechts. J. J. (2000). Broad spectrum diffusion model for room acoustics ray-tracing algorithms. J. Acoust. Soc. Am. 107(4), 2068-2081.

[14] Zwicker, E. and Fastl, H. (1999). Psychoacoustics, Springer-Verlag, 2nd edition.